Motional Averaging of Proton Nuclear Overhauser Effects in Proteins. Predictions from a Molecular Dynamics Simulation of Lysozyme†

E. T. Olejniczak,‡⊥ C. M. Dobson,*†∥ M. Karplus,*‡ and R. M. Levy§

Contribution from the Department of Chemistry, Harvard University, Cambridge, Massachusetts 02138, and Department of Chemistry, Rutgers, The State University of New Jersey, New Brunswick, New Jersey 08903. *Received July 5, 1983*

Abstract: A molecular dynamics simulation has been used to explore the effects of fast internal motions on the ^1H NMR relaxation behavior of lysozyme. It is shown that cross-relaxation rates, which are experimentally accessible from the time development of nuclear Overhauser effects (NOEs), are reduced by motional averaging on a picosecond time scale. Factors influencing the magnitude of these changes have been explored, including the degree of correlation of side-chain torsion angle fluctuations. More general effects on NOEs were examined by multispin simulation techniques. The internal motions altered the magnitude of specific NOEs by as much as a factor of 2. However, at the present level of experimental knowledge, it is difficult to separate these effects from the results expected for an internally rigid structure with a shorter correlation time for overall tumbling. The results show that in general, the picosecond internal motions examined here have little effect on estimates of distances obtained from NOE measurements.

A variety of experimental and theoretical techniques are now being applied to the study of internal motions of proteins.[1,2] Nuclear magnetic resonance (NMR) measurements are particularly useful because they can provide specific information about both the amplitudes and time scales of these motions.[3] Relaxation times and nuclear Overhauser effects (NOEs) for ^{13}C are of special interest because their relaxation is dominated by the fluctuating dipolar interactions between the ^{13}C nucleus and the directly bonded proton.[4] The relaxation parameters can be related to the motional averaging of the dipolar interaction and hence to the motional behavior of individual groups.[5,6] The available studies have demonstrated that large-amplitude fluctuations can occur on nanosecond or subnanosecond time scales. Furthermore, comparisons with the results of molecular dynamics simulations have shown that the averaging due to picosecond fluctuations can have a significant effect on the relaxation times of both protonated and nonprotonated nuclei.[7-9] More recently, ^1H NOEs have been used to obtain motional information for proteins.[10] Averaging effects due to atomic fluctuations decrease the magnitude of the cross-relaxation rates in the same way that they increase the ^{13}C relaxation times.

Molecular dynamics trajectories of proteins permit the direct calculation of the time correlation functions required for determining the effects of picosecond motional averaging. This approach has proven to be useful in ^{13}C NMR for examining motional models used in the analysis of data and as an aid in the interpretation of experiments.[7-9] A similar study of the effects of internal motions on ^1H NOEs is highly desirable. Such a study could test the methods used to interpret the NMR measurements. In particular, it could examine the effect that motional averaging has on structural information obtained from NOE data. Of considerable importance is the effect that hindered motions of residues in the interior of the protein have on the ^1H NOE data. Because of excluded volume effects, any large-magnitude motions that occur are a consequence of collective effects involving a number of neighboring groups.[11,12] Most models used to interpret relaxation data treat each degree of freedom as independent. This assumption is not valid in the protein interior,[11] although it is appropriate for the behavior of exterior side chains.[8]

The present study is limited to the effect of subnanosecond fluctuations on the NOE values. It does not consider the contributions of internal motions with longer time scales because of the limited length of the available dynamics runs. Fluctuations on slower time scales will further decrease the magnitude of the relaxation rates for the spectrometer frequencies and tumbling times under consideration. Many of the effects that internal motions can have on NOEs may, however, be demonstrated by considering only the effects of the fast picosecond motions. We have focused our study on several residues found in the hydrophobic box region of lysozyme for which there are assigned resonances and detailed experimental evaluations of NOEs.[10,13] This region is in the interior of the protein, and the motions are expected to be governed by van der Waals interactions, which are well modeled by the empirical potentials used in the dynamics simulations. The following section outlines the theory for the relaxation rates which govern the NOEs in the presence of fast internal motions as well as overall protein tumbling. Simplifications in the theory are shown to be possible when the time scale of the internal motion is much faster than the tumbling time. We then compare the NOE results from a static structure to those obtained with the molecular dynamics trajectories and outline the conse-

† Supported in part by grants from the National Science Foundation and the National Institutes of Health.

‡ Harvard University.

§ Rutgers, The State University of New Jersey.

⊥ Present address: Massachusetts Institute of Technology, National Magnet Lab, Cambridge, MA 02138.

∥ Present address: Inorganic Chemistry Laboratory, Oxford University, Oxford O81 3QR, England.

(1) M. Karplus and J. A. McCammon, *CRC Crit. Rev. Biochm.*, **9**, 293 (1981).

(2) F. R. N. Gurd and M. Rothgeb, *Adv. Protein Chem.*, **33**, 74 (1979).

(3) R. E. London in "Magnetic Resonance in Biology", Vol. 1, J. S. Cohen, Ed., Wiley, New York, 1980, p 1.

(4) A. A. Allerhand, D. Doddrell, and R. Komorski, *J. Chem. Phys.*, **55**, 189 (1971).

(5) G. C. Levy, D. E. Nelson, R. Schwartz, and J. Hochmann, *J. Am. Chem. Soc.*, **100**, 410 (1978).

(6) R. J. Wittebort, M. Rothgeb, A. Szabo, and. F. R. N. Gurd, *Proc. Natl. Acad. Sci. U.S.A.* **76**, 1059 (1979).

(7) R. M. Levy, C. M. Dobson, and M. Karplus, *Biophys. J.*, **39**, 107 (1982).

(8) R. M. Levy, M. Karplus, and P. G. Wolynes, *J. Am. Chem. Soc.*, **103**, 5998 (1981).

(9) R. M. Levy, M. Karplus, and J. A. McCammon, *J. Am. Chem. Soc.*, **103**, 994 (1981).

(10) E. T. Olejniczak, F. M. Poulsen, and C. M. Dobson, *J. Am. Chem. Soc.*, **103**, 6574 (1981).

(11) W. F. Gunsteren and M. Karplus, *Biochemistry*, **21**, 2259 (1982).

(12) S. Swaminathan, T. Ichiye, W. van Gunsteren, and M. Karplus, *Biochemistry*, **21**, 5230 (1982).

(13) F. M. Poulsen, J. C. Hoch, and C. M. Dobson, *Biochemistry*, **19**, 2597 (1980).

(14) J. H. Noggle and R. E. Shirmer, "The Nuclear Overhauser Effect", Academic Press, New York, 1971.

(15) A. Abragam, "The Principles of Nuclear Magnetism", Clarendon, Press, Oxford, 1961.

0002-7863/84/1506-1923$01.50/0

quences of internal motions for the interpretation of NOE measurements. Finally, the conclusions of the present study are summarized.

Theory

(a) Motional Averaging of Relaxation Rates. In this section, we present the theory that describes the effect of internal motions on relaxation rates. We then outline the use of molecular dynamics results for calculating picosecond averaging effects. Finally we consider a model that treats the fluctuations about each side-chain bond as independent; this product approximation is compared to the results from the full dynamics trajectory.

For a system of dipolar-coupled spins with no cross-correlation, the spin–lattice relaxation is governed by coupled differential equations of the form[14,15]

$$\frac{d(I_z(t) - I_0)_i}{dt} = -\rho_i(I_z(t) - I_0)_i - \sum_{i \neq j} \sigma_{ij}(I_z(t) - I_0)_j \quad (1)$$

where $I_z(t)_j$ and I_{0j} are the z components of the magnetization of nucleus j, ρ_i is the direct-relaxation rate of proton i, and σ_{ij} is the cross-relaxation rate between protons i and j. For dipolar relaxation ρ_i and σ_{ij} can be defined in terms of spectral densities as

$$\rho_i = \frac{6\pi}{5}\gamma^4\hbar^2\sum_{j \neq i}[(1/3)J_{ij}(0) + J_{ij}(\omega) + 2J_{ij}(2\omega)] \quad (2)$$

and

$$\sigma_{ij} = \frac{6\pi}{5}\gamma^4\hbar^2[2J_{ij}(2\omega) - (1/3)J_{ij}(0)] \quad (3)$$

where the subscripts ij refer to the pairwise interaction between protons i and j, γ is the proton gyromagnetic ratio, and ω is the ^1H Larmor frequency. The spectral density functions, $J_{ij}(\omega)$, can be expressed as Fourier cosine transforms of the correlation functions[16]

$$J^n_{ij}(\omega) = \int_0^\infty \left\langle \frac{Y^2_n(\theta_{lab}(t)\phi_{lab}(t))Y^{2*}_n(\theta_{lab}(0)\phi_{lab}(0))}{r_{ij}^3(0)r_{ij}^3(t)} \right\rangle \cos(\omega t)\, dt \quad (4)$$

where $Y^2_n(\theta(t)\phi(t))$ are second-order spherical harmonics and the angular brackets represent a correlation function. The quantities $\theta_{lab}(t)$ and $\phi_{lab}(t)$ are the polar angles at time t of the internuclear vector between protons i and j with respect to the external magnetic field and r_{ij} is the interproton distance. It is clear from eq 3 that σ_{ij}, the pairwise cross-relaxation rate, is the quantity that can be interpreted most easily to obtain structural and motional information because only one proton–proton interaction is involved; ρ_i as given in eq 2 includes a sum over a number of such interactions.[10]

If the internal motions are uncorrelated with the overall molecular tumbling, the time correlation function appearing in eq 4 can be separated into contributions from molecular tumbling and internal motions as[7,8]

$$\left\langle \frac{Y^2_m(\theta_{lab}(t)\phi_{lab}(t))Y^{2*}_m(\theta_{lab}(0)\phi_{lab}(0))}{r_{ij}^3(0)r_{ij}^3(t)} \right\rangle = \sum_{aa'=-2}^{2} \langle D^2_{ma}(\Omega_1(t))D^{2*}_{ma'}(\Omega_1(0))\rangle \times \left\langle \frac{Y^2_a(\theta_{mol}(t)\phi_{mol}(t))Y^{2*}_{a'}(\theta_{mol}(0)\phi_{mol}(0))}{r_{ij}^3(0)r_{ij}^3(t)} \right\rangle \quad (5)$$

The D^2_{ma} are Wigner rotation matrix elements.[17] The $\Omega_1(t)$ are the Euler angles that transform from the laboratory frame to the molecular frame and $\theta_{mol}(t)$ and $\phi_{mol}(t)$ are the spherical polar angles relating the interproton vector to the fixed molecular frame. For an isotropically tumbling molecule, the time correlation function has been shown to decay as a single exponential of the form[18]

$$\langle D^2_{ma}(\Omega_1(t))D^{2*}_{ma'}(\Omega_1(0))\rangle = \frac{\exp(-t/\tau_0)}{5}\delta_{aa'} \quad (6)$$

where τ_0 is the correlation time for molecular tumbling. Introducing this result into eq 5 gives

$$\left\langle \frac{Y^2_m(\theta_{lab}(t)\phi_{lab}(t))Y^{2*}_m(\theta_{lab}(0)\phi_{lab}(0))}{r_{ij}^3(0)r_{ij}^3(t)} \right\rangle = \frac{\exp(-t/\tau_0)}{5}\sum_{a=-2}^{2}\left\langle \frac{Y^2_a(\theta_{mol}(t)\phi_{mol}(t))Y^{2*}_a(\theta_{mol}(0)\phi_{mol}(0))}{r_{ij}^3(0)r_{ij}^3(t)} \right\rangle = \frac{\exp(-t/\tau_0)}{4\pi}\langle A(0)A(t)\rangle \quad (7)$$

where $\langle A(0)A(t)\rangle$ is referred to as the internal motion correlation function. For a rigid molecule undergoing only isotropic tumbling, the spherical harmonics on the right-hand side of eq 7 can be summed and substituted into eq 4 to yield

$$J_{ij}(\omega) = \frac{1}{4\pi r_{ij}^6}\left[\frac{\tau_0}{1 + (\omega\tau_0)^2}\right] \quad (8)$$

If internal motion is occurring, however, the ensemble average over molecular conformations on the right-hand side of eq 7 needs to be evaluated.

(b) Molecular Dynamics Simulations and Motional Averaging. The molecular dynamics trajectory used in this investigation was obtained from a 33-ps simulation of lysozyme. The method employed in the simulations has been described previously.[19] Protons were not included explicitly but were taken into account by the extended-atom technique in which the mass and van der Waals radii of the directly bonded heavy atoms are adjusted to compensate for the protons.[11] The average temperature during the dynamics run was 304 K. Details of the simulation and its analysis will be reported elsewhere.[20] Three hundred and thirty coordinate sets separated by 0.1 ps were selected from the trajectory and used in the analysis.

For each configuration, protons were generated in standard configurations using a C–H bond length of 1.08 Å.[21] Methyl group protons were constructed in a staggered configuration. To obtain a static structure with which the dynamics results could be compared, protons were generated onto the average heavy-atom coordinates of the dynamics run. The average coordinates of the heavy atoms were energy minimized for 100 steps to remove unreasonable internal coordinate values[19] before being used to generate the proton coordinates. The root-mean-square difference between the energy-minimized and average heavy-atom structure was 0.149 Å. Relaxation rates and distances obtained from the average structure, assumed rigid, were compared with the averages and correlation functions computed from the 330 coordinate sets of the trajectory. The motions modeled by the trajectory are dominated by high-frequency fluctuations.[12] These fast motions were nearly homogeneous for the dynamics run for the residues studied here; i.e., a comparison of interproton distances and dihedral fluctuations for the two halves of the run (the first 16.5 ps and the second 16.5 ps) gave very similar results. It is therefore expected that the results were not significantly influenced by any statistically rare events.

(16) I. Solomon, *Phys. Rev.*, **99**, 559 (1955).
(17) D. M. Brink and G. R. Satchler, "Angular Momentum", Oxford University Press, Oxford, 1971.
(18) D. Wallach, *J. Chem. Phys.*, **47**, 5258 (1967).
(19) B. R. Brooks, R. E. Bruccoleri, B. D. Olafson, D. J. States, S. Swaminathan, and M. Karplus, *J. Comput. Chem.*, **4**, 187 (1983).
(20) T. Ichiye, B. Olafson, and M. Karplus, to be submitted for publication.
(21) J. C. Hoch, C. M. Dobson, and M. Karplus, *Biochemistry*, **21**, 1118 (1982).

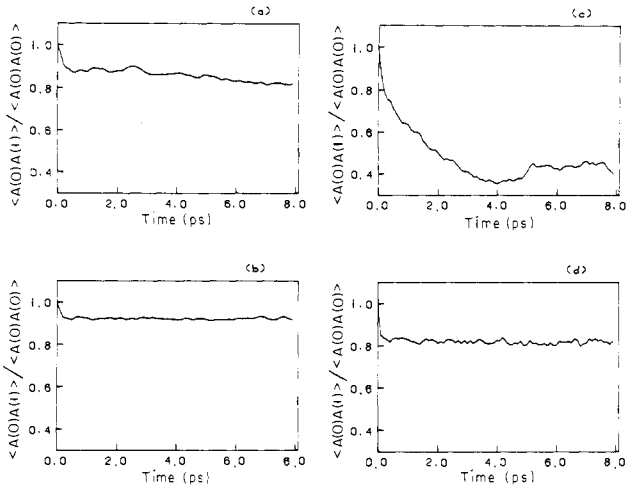

Figure 1. Decay of the fixed-distance interproton internal motion correlation function for intraresidue vectors on the four hydrophobic box residues studied (eq 7): (a) Trp-28 $H^{\beta 3}$–$H^{\eta 3}$, (b) Trp-108 $H^{\beta 3}$–$H^{\eta 3}$, (c) Met-105 $H^{\gamma 1}$–$H^{\gamma 2}$, (d) Ile-98 $H^{\gamma 11}$–$H^{\gamma 12}$.

The results of molecular dynamics simulations permit direct evaluation of the internal motion correlation function.[19] The decay of several internal motion correlation functions obtained from the dynamics trajectory is shown in Figure 1. Because the motions in the interior of a protein tend to be restricted by van der Waals interactions, the correlation functions generally do not decay to zero during the dynamics trajectory.[7,9] Instead, after a rapid initial decay a plateau value is reached in τ_p picoseconds, where τ_p is a time short in comparison with the length of the trajectory, so that $\tau_p\omega \ll 1.0$. This is true for three of the four correlation functions in Figure 1; the fourth, which corresponds to Met-105, also appears to have approached a plateau, but its fluctuations are too large to be certain. For the cases where a plateau value is reached, the internal motion correlation function is equal to the equilibrium orientational distribution for the dynamics trajectory such that[7,8]

$$\frac{4\pi}{5}\sum_{n=-2}^{2}\left\langle \frac{Y^2{}_n(\theta_{mol}(t)\phi_{mol}(t))Y^{2*}{}_n(\theta_{mol}(0)\phi_{mol}(0))}{r_{ij}{}^3(0)r_{ij}{}^3(t)}\right\rangle = \frac{4\pi}{5}\sum_{n=-2}^{2}\left|\left\langle \frac{Y^2{}_n(\theta_{mol}(0)\phi_{mol}(0))}{r_{ij}{}^3}\right\rangle\right|^2 = S^2\langle r_{ij}{}^{-6}\rangle \qquad (t > \tau_p) \quad (9)$$

Equation 9 provides the definition for a generalized order parameter, S^2, for the motion of the ^1H_i–^1H_j vector. This order parameter is the same as that defined previously for ^{13}C relaxation.[7,8,22] Both angular and radial averaging due to internal motions will decrease the order parameter from the value of unity, obtained when no internal motion exists. To combine the result of eq 9 with eq 7 it is necessary that the plateau value be reached rapidly in comparison to the overall tumbling rate. Treating the effect of the fast picosecond motions as a constant for $t > \tau_p$, the cosine Fourier transform of eq 7 can be evaluated by breaking the integral into two parts; we have

$$J_{ij}(\omega) = \frac{1}{4\pi}\int_0^\infty \langle A(0)A(t)\rangle \exp(-t/\tau_0)\cos(\omega t)\,dt = \frac{1}{4\pi}\int_0^{\tau_p}[\langle A(0)A(t)\rangle - S^2\langle r_{ij}{}^{-6}\rangle]\exp(-t/\tau_0)\cos(\omega t)\,dt + \frac{1}{4\pi}\int_0^\infty S^2\langle r_{ij}{}^{-6}\rangle \exp(-t/\tau_0)\cos(\omega t)\,dt \quad (10)$$

where $S^2\langle r_{ij}{}^{-6}\rangle$ was substituted for $\langle A(0)A(t)\rangle$ when $t > \tau_p$. In the present cases, τ_p is ony a few picoseconds and the plateau value of the correlation function, $S^2\langle r_{ij}{}^{-6}\rangle$, is always much greater than zero. Under these conditions the contribution of the first integral to the spectral density function is negligible. This can be seen by approximating both cos (ωt) and exp($-t/\tau_0$) by 1 for ($t < \tau_p < \tau_0$) in eq 10. The first integral is then approximately

$$\int_0^{\tau_p}[\langle A(t)A(0)\rangle - S^2\langle r_{ij}{}^{-6}\rangle]\,dt \qquad (11)$$

For an exponential decrease in the internal motion correlation functions found in this and other studies using dynamics trajectories of proteins, the integral is less than $\tau_p[\langle A(0)A(0)\rangle - S^2\langle r_{ij}{}^{-6}\rangle]/2$, which is the area of the triangle of base τ_p and height $[\langle A(0)A(0)\rangle - S^2\langle r_{ij}{}^{-6}\rangle]$. For $\tau_p < 33$ ps, $\tau_0 = 10$ ns, and a spectrometer frequency of 500 MHz, the area of this triangle is less than 2% of the second term in eq 10 for all of the cases studied in this work. Thus this contribution to the spectral density function has been neglected here. The Fourier transform of the second integral in eq 10 gives a spectral density function that is scaled by the factor $S^2\langle r_{ij}{}^{-6}\rangle$; that is,

$$J(\omega) = \frac{S^2\langle r_{ij}{}^{-6}\rangle}{4\pi}\left[\frac{\tau_0}{1+(\omega\tau_0)^2}\right] \qquad (12)$$

Equation 12 provides the basis for calculating the spectral density functions from the molecular dynamics simulation.

For the general case, the first integral may not be negligible relative to the second. The analysis of such motions and their contribution to NMR relaxation times have been discussed by Lipari and Szabo.[22,23] In an appendix we compare the present analysis of the effects of the fast motions from the dynamics trajectory to the method of analysis suggested by Lipari and Szabo.

(c) Product Approximation for Relaxation. The torsion angle fluctuations about side-chain bonds of a given residue are known to be highly correlated in the interior of a protein.[11,12] The effect of this on the motional averaging of relaxation rates can be determined by comparing the correlation function obtained directly from the dynamics trajectory to that obtained by assuming that the side-chain torsion angle fluctuations about each side-chain bond are independent. Including the side-chain conformation explicitly in eq 7, we obtain[8,18]

$$\left\langle \frac{Y^2{}_n(\theta_{lab}(t)\phi_{lab}(t))Y^{2*}{}_n(\theta_{lab}(0)\phi_{lab}(0))}{r_{ij}{}^3(0)r_{ij}{}^3(t)}\right\rangle = \frac{\exp(-t/\tau_0)}{5}\sum_{nbb'cc'dd'}\left\langle D^2{}_{nb}(\Omega_1(t))D^{2*}{}_{nb'}(\Omega_1(0))D^2{}_{bc}(\Omega_2(t))\times D^{2*}{}_{b'c'}(\Omega_2(0))D^2{}_{cd}(\Omega_3(t))D^{2*}{}_{c'd'}(\Omega_3(0))\times \frac{Y^2{}_{d'}(\theta_3(t)\phi_3(t))Y^{2*}{}_{d'}(\theta_3(0)\phi_3(0))}{r_{ij}{}^3(0)r_{ij}{}^3(t)}\right\rangle \quad (13)$$

where Ω_1 relates the molecule-fixed axis to the first local axis system which has its z axis along N–C^α, Ω_2 relates the first axis to the second with its z axis along C^α–C^β, and Ω_3 relates the second axis to the third with its z axis along C^β–C^γ; additional product terms would be introduced as the transformation moves out along the side chain of the residue being studied. The angles $\theta_3(t)$ and $\phi_3(t)$ are the polar angles of the interproton vector in the final axis system. If the motions are uncorrelated, the averages about each bond can be taken separately to give for the right-hand side of eq 13

$$\frac{\exp(-t/\tau_0)}{5}\sum_{nbb'cc'dd'}\langle D^2{}_{nb}(\Omega_1(t))D^{2*}{}_{nb'}(\Omega_1(0))\rangle \times \langle D^2{}_{bc}(\Omega_2(t))D^{2*}{}_{b'c'}(\Omega_2(0))\langle D^2{}_{cd}(\Omega_3(t))D^{2*}{}_{c'd'}(\Omega_3(0))\rangle \times \left\langle \frac{Y^2{}_{d'}(\theta_3(t)\phi_3(t))Y^{2*}{}_{d'}(\theta_3(0)\phi_3(0))}{r_{ij}{}^3(0)\,r_{ij}{}^3(t)}\right\rangle \quad (14)$$

From the behavior of correlation functions at long times

(22) G. Lipari and A. Szabo, *J. Am. Chem. Soc.*, **104**, 4546 (1982).

(23) G. Lipari and A. Szabo, *J. Am. Chem. Soc.*, **104**, 4559 (1982).

$$\lim_{t\to\infty} \langle A(t)B(0)\rangle = \langle A\rangle\langle B\rangle$$

the long-time behavior of eq 14 can be rewritten as[8]

$$\frac{\exp(-t/\tau_0)}{5}\left|\sum_{nbcd}\langle D^2_{nb}(\Omega_1)\rangle\langle D^2_{bc}(\Omega_2)\rangle \times \langle D^2_{cd}(\Omega_3)\rangle\left\langle \frac{Y^2_d(\theta_3(0)\phi_3(0))}{r_{ij}^3}\right\rangle\right|^2 \quad (15)$$

The cosine transform of eq 15 gives the spectral density function at long times, assuming uncorrelated motion about the bonds.

(d) Multispin Simulations of the NOE. Selective saturation of a transition in a dipolar-coupled spin system results in intensity changes in the other transitions. The intensity changes are called NOEs.[14] Time-dependent NOEs can be observed, for example, by measuring the change in intensity of the resonances as a function of the length of time that the saturating radio-frequency field is present. The change in the resonance intensity of spin i caused by irradiation of j can be used to define a time-dependent nuclear Overhauser enhancement factor

$$\eta_i(t) = \frac{(I_z(t) - I_0)_i}{I_{0i}}$$

In a large molecule like a protein the observed $\eta_i(t)$ will depend not only on the cross-relaxation rate σ_{ij} coupling i to the irradiated proton j (eq 3) but also on the relaxation rates of the other spins in the system. It is therefore necessary to consider multispin effects in order to interpret the observed NOEs. Such multispin treatments have been described earlier[24,25] and are used here to simulate the NOEs.

Each multispin simulation involved a partial set of the protons in the protein. The first 20 protons or methyl groups included in a set were those with the shortest distances to the irradiated proton in the proton coordinate set derived from the average coordinates of the dynamics run. To minimize the effect of a limited proton set on the calculated NOEs we also included the three nearest neighbors of each of the first 20 protons in the set. The ρ values (eq 2) for these additional protons included contributions from their three nearest neighbors even if their neighbors were not explicitly included in the proton set. Each resulting proton set included at least all of the protons within 4.5 Å of the irradiated proton. This approach assumes that no significant amount of magnetization which leaves the proton set will return through cross-relaxation effects. To test the assumption, proton sets of various sizes were included in the NOE simulations. It was found that proton sets that are larger than those described above did not cause significant differences in the calculated NOEs of the 20 closest protons.

A complication in the analysis is the treatment of methyl groups. Here we make use of the fact that the correlation time for overall tumbling ($\tau_0 \approx 10$ ns)[26,27] is much slower than the correlation times for methyl rotation, which are in the range of 20–200 ps.[28] In the NOE simulations it was assumed that the methyl rotation can be modeled by fast random jumps between three methyl proton sites. The spectral density function obtained between a methyl proton and a non-methyl proton for an otherwise rigid protein tumbling in solution is then given by[29]

$$J_{ij}(\omega) = \frac{1}{5}\frac{\tau_0}{1 + (\omega\tau_0)^2}\sum_{n=-2}^{2}\left|\frac{1}{3}\sum_{i=1}^{3}\frac{Y^2_n(\theta_{\mathrm{mol}}{}^i\phi_{\mathrm{mol}}{}^i)}{r_{ij}^3}\right|^2 \quad (16)$$

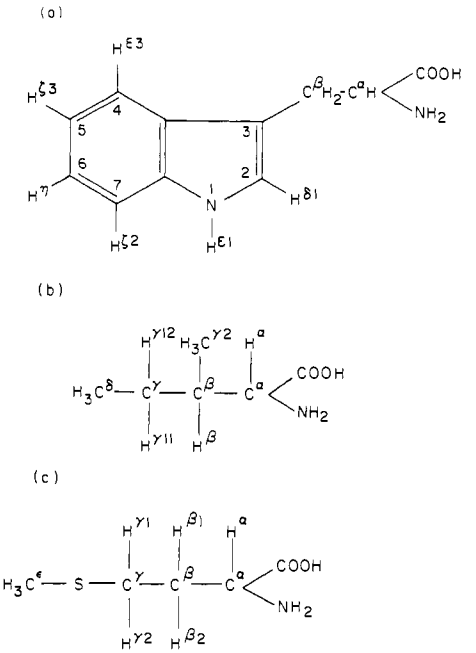

Figure 2. Tryptophan (a), isoleucine (b), and methionine (c) amino acids showing the labeling of the hydrogen atoms.

where $\theta_{\mathrm{mol}}{}^i$ and $\phi_{\mathrm{mol}}{}^i$ are the polar angles in the molecular frame of the internuclear vector of length r_{ij} between proton j and each of the three methyl protons in the rigid protein structure.

Since methyl rotation is not considered explicitly in the dynamics simulation, a generalized form of eq 16 was used to introduce the effect of motion of the methyl group that occurs in addition to its internal rotations. It is assumed that the picosecond motions modeled by the simulation and the methyl rotations are uncoupled. Then the spectral densities can be approximated by using the motionally averaged values of the spherical harmonics obtained from the dynamics simulation. This approach replaces eq 16 by the expression

$$J_{ij}(\omega) = \frac{1}{5}\frac{\tau_0}{1 + (\omega\tau_0)^2}\sum_{n=-2}^{2}\left|\frac{1}{3}\sum_{i=1}^{3}\left\langle \frac{Y^2_n(\theta_{\mathrm{mol}}{}^i\phi_{\mathrm{mol}}{}^i)}{r_{ij}^3}\right\rangle\right|^2 \quad (17)$$

where now the average of $\theta_{\mathrm{mol}}{}^i$, $\phi_{\mathrm{mol}}{}^i$, and $r_{ij}{}^3$ over the entire dynamics simulation is used, as indicated by the angular bracket.

Results and Discussion

In this section we describe first the effect of the internal motions on the relaxation rates and then consider the implications for the interpretation of NOE measurements. We focus on the behavior of protons on four residues in a region called the hydrophobic box of lysozyme:[13,30] they are Trp-28, Trp-108, Ile-98, and Met-105; the protons are named according to convention[31] (see Figure 2).

(a) Cross-Relaxation Rates. Intraresidue Fixed-Distance Interactions. Internal motion interproton vector correlation functions for pairs of protons on the four residues studied are shown in Figure 1; these examples are for proton pairs where the interproton distances are fixed by the geometry of the residue. A rapid loss of correlation is observed in the first few picoseconds. The correlation functions are similar to those reported for the $^{13}C-^1H$ vectors from dynamic simulations of BPTI.[7,9] Plateau values were reached for the proton vectors of Ile-98 and Trp-108 in less than 1 ps. This indicates that only very fast motions are involved. For Trp-28 there is a rapid decay of similar magnitude, but there is an additional slow loss of correlation over the 8 ps for which the correlation function was calculated. This suggests that motions

(24) C. M. Dobson, E. T. Olejniczak, F. M. Poulsen, and R. G. Ratcliffe, *J. Magn. Reson.*, **48**, 97 (1982).
(25) A. A. Bothner-By and J. H. Noggle, *J. Am. Chem. Soc.*, **101**, 5152 (1979).
(26) S. B. Dubin, N. A. Clark, and G. B. Benedek, *J. Chem. Phys.*, **54**, 5158 (1971).
(27) K. Dill and A. Allerhand, *J. Am. Chem. Soc.*, **101**, 4376 (1979).
(28) E. R. Andrew, W. S. Hinshaw, and M. G. Hutchins, *J. Magn. Reson.* **15**, 196 (1974).
(29) J. Tropp, *J. Chem. Phys.*, **72**, 6035 (1980).
(30) F. C. C. Blake, N. L. Johnson, A. G. Main, T. C. A. North, D. C. Phillips, and V. R. Sarma *Proc. R. Soc. London, Ser. B*, **167**, 378 (1967).
(31) IUPAC–IUB Commision on Biochemical Nomenclature, *J. Mol. Biol.*, **52**, 1 (1970).

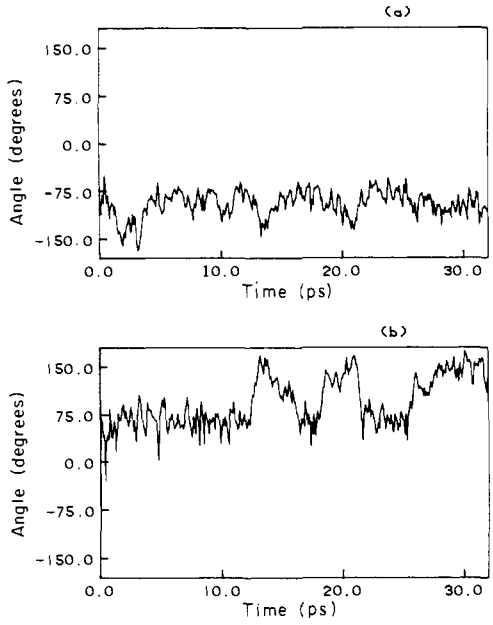

Figure 3. Torsion angle fluctuations for the Met-105 side chain calculated from the 33-ps dynamics simulation of lysozyme: (a) χ_1, (b) χ_2.

Table I. Intraresidue Order Parameters (Fixed Geometry)

^{1}H–^{1}H vector	$S^{2\,a}$
Trp-28	
$H^{\epsilon 3}$–$H^{\zeta 3}$	0.86
$H^{\zeta 3}$–$H^{\eta 3}$	0.83
$H^{\eta 3}$–$H^{\zeta 2}$	0.79
$H^{\zeta 2}$–$H^{\epsilon 1}$	0.80
$H^{\epsilon 1}$–$H^{\delta 1}$	0.88
Trp-108	
$H^{\epsilon 3}$–$H^{\zeta 3}$	0.92
$H^{\zeta 3}$–$H^{\eta 3}$	0.91
$H^{\eta 3}$–$H^{\zeta 2}$	0.90
$H^{\zeta 2}$–$H^{\epsilon 1}$	0.93
$H^{\epsilon 1}$–$H^{\delta 1}$	0.91
Ile-98	
$H^{\gamma 11}$–$H^{\gamma 12}$	0.82
Met-105	
$H^{\beta 1}$–$H^{\beta 2}$	0.69
$H^{\gamma 1}$–$H^{\gamma 2}$	0.35

[a] The value of the order parameter obtained from averaging over the 33-ps trajectory; for a rigid molecule $S^2 = 1.0$.

on the time scale of several picoseconds are also contributing to the motional averaging. The interproton vectors of Met-105 have the largest decay over the time range investigated; as Figure 1 indicates, a plateau value apparently is reached though the fluctuations in the correlation function are too large to be certain. The behavior of Met-105 can be understood by looking at the torsion angle fluctuations. Fluctuations about two different side-chain conformations ($\chi_2 \approx 60°$ and $\chi_2 \approx 180°$) occur for this residue (Figure 3); jumps between the two conformations are on the time scale of several picoseconds. For Trp-28, Trp-108, and Ile-98, the fluctuations are about only a single side-chain conformation.

As the interproton distances are fixed by the geometry of a residue in these cases, the picosecond averaging is due only to the reorientation of the interproton vector. The effects of motional averaging can thus be described directly by the order parameter S^2, given by eq 9, which scales the cross-relaxation rates. Values of S^2, derived from the dynamics simulation for the fixed-distance interactions on the four residues, are listed in Table I. It is evident that motional averaging causes a significant decrease in the magnitudes of the cross-relaxation rates from the values that would be expected for isotropic tumbling of a rigid molecule. Large differences in the degree of averaging are observed for the four residues; the decrease in the cross-relaxation rates varies from 10%

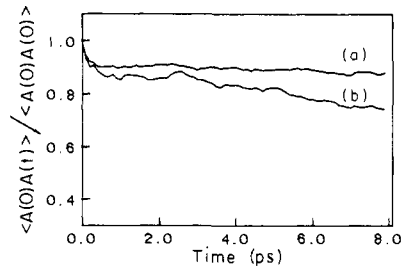

Figure 4. Comparison of the internal motion correlation function for (a) $H^{\epsilon 1}$–$H^{\delta 1}$ and (b) $H^{\eta 3}$–$H^{\zeta 2}$ in Trp-28.

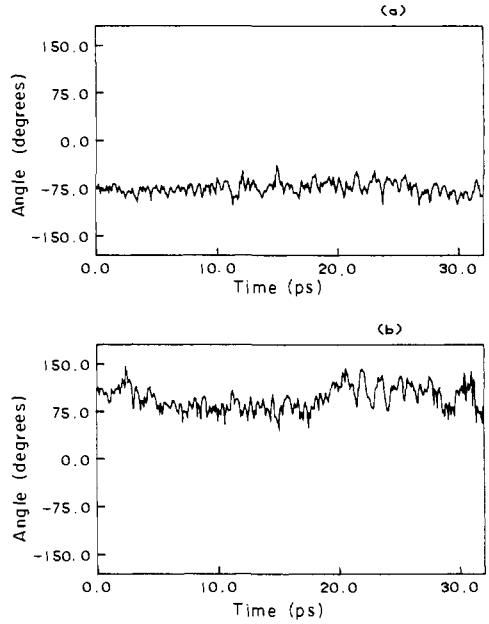

Figure 5. Torsion angle fluctuations for the Trp-28 side chain calculated from the 33-ps dynamics simulation: (a) χ_1, (b) χ_2.

or less for all the proton pairs of Trp-108 to as much as 65% for one of the pairs of Met-105. The large effect observed for Met-105 arises from the jumps between different torsion angle conformations described above (see Figure 3). As one might expect, S^2 for the β protons of Met-105, which have less conformational freedom, is larger than S^2 for the γ protons.

Although all of the order parameters for a given tryptophan residue are similar, some variation does exist. An example is the difference between $H^{\epsilon 1}$–$H^{\delta 1}$ ($S^2 = 0.88$) and $H^{\eta 3}$–$H^{\zeta 2}$ ($S^2 = 0.79$) of Trp-28. Internal motion correlation functions for these two interactions are shown in Figure 4. The difference in behavior of the internal motion correlation function is due to the dependence of the effects of motional averaging on the orientation of the interproton vector.[32,33] The $H^{\epsilon 1}$–$H^{\delta 1}$ interproton vector is nearly parallel to the C^{β}–C^{γ} rotation axis so that rotation about that axis has only a small effect on its averaging. In contrast, $H^{\eta 3}$–$H^{\zeta 2}$ is averaged by rotation about both C^{α}–C^{β}(χ_1) and C^{β}–C^{γ}(χ_2). The slow decay of the internal motion correlation function for the $H^{\eta 3}$–$H^{\zeta 2}$ interaction (see Figure 4) is a result of the gradual change in the torsion angle about C^{β}–C^{γ}. As is evident in Figure 5, there is a low-frequency ($\approx$10 ps) variation in χ_2, superimposed on its fast torsion angle fluctuations.

Other Intraresidue Interactions. For intraresidue interactions whose distances are not fixed by the geometry of the residue, rotations about side-chain torsional angles change the average distance between protons as well as the orientation of the interproton vector. The correlation functions for these effects also decay rapidly to a plateau value, with most of the decay occurring in the first 8 ps. Some of the variable-distance intraresidue inter-

(32) R. E. London and J. Avitable, *J. Am. Chem. Soc.*, **100**, 7159 (1978).
(33) R. J. Wittebort and A. Szabo, *J. Chem. Phys.*, **69**, 1722 (1978).

Table II. Variable-Distance Intraresidue Interactions[a,b]

^{1}H-^{1}H vector	S^2	r^{-6}_{av}	$\langle r^{-6}\rangle$	$S^2\langle r^{-6}\rangle / r^{-6}_{av}$
Ile-98				
$H^{\gamma 11}$-H^{β}	0.91	0.0014	0.0015	1.00
$H^{\gamma 11}$-H^{α}	0.87	0.0021	0.0021	0.86
$H^{\gamma 12}$-H^{β}	0.89	0.0024	0.0025	0.92
$H^{\gamma 12}$-H^{α}	0.84	0.0036	0.0040	0.94
Met-105				
$H^{\beta 1}$-H^{α}	0.86	0.0015	0.0016	0.93
$H^{\beta 1}$-$H^{\gamma 1}$	0.51	0.0026	0.0035	0.69
$H^{\beta 1}$-$H^{\gamma 2}$	0.70	0.0015	0.0019	0.87
$H^{\beta 2}$-H^{α}	0.85	0.0024	0.0026	0.92
$H^{\beta 2}$-$H^{\gamma 1}$	0.48	0.0075	0.0064	0.41
$H^{\beta 2}$-$H^{\gamma 2}$	0.64	0.0025	0.0034	0.88

[a] For definition of the order parameter S^2 see eq 9; for a rigid molecule $S^2 = 1.0$. [b] Values of r^{-6}_{av} are obtained from the static structure described in text; $\langle r^{-6}\rangle$ are averages over the 33 ps of the trajectory. All distances are in Å.

Table III. Interresidue Interactions[a,b]

^{1}H-^{1}H vector	S^2 [a]	r^{-6}_{av}	$\langle r^{-6}\rangle$	$S^2\langle r^{-6}\rangle / r^{-6}_{av}$
Trp-28 $H^{\zeta 3}$-Val-92 H^{α}	0.59	0.0018	0.0020	0.67
Trp-108 $H^{\zeta 3}$-Met-105 $H^{\gamma 2}$	0.47	0.0124	0.0195	0.74
Trp-108 $H^{\zeta 3}$-Met-105 H^{α}	0.59	0.0032	0.0037	0.69
Met-105 $H^{\beta 1}$-Tyr-23 $H^{\epsilon 1}$	0.56	0.0026	0.0037	0.81
Ile-98 $H^{\gamma 12}$-Cys-76 $H^{\beta 2}$	0.60	0.0054	0.0071	0.80
Ile-98 $H^{\gamma 12}$-Cys-76 $H^{\beta 1}$	0.68	0.0038	0.0041	0.74

[a] See footnote *a* of Table II. [b] See footnote *b* of Table II.

actions for Met-105 and Ile-98 are listed in Table II; see Figure 2 for the proton labels. The order parameters S^2 for these protons are comparable to those found for the fixed-distance interactions found in Table I. Examination of the effects of motional averaging here must, however, include a consideration of the effects of interproton distance fluctuations as well as fluctuation in the orientation defined by S^2. Because of the strong distance dependence of the interactions, small differences in the average distance can cause large changes in the magnitude of the cross-relaxation rate. In the table, values of r_{ij}^6 obtained from generating protons onto the average heavy-atom coordinate set (r^{-6}_{av}) are compared to the values of $\langle r^{-6}\rangle$ obtained from the simulation. In most cases the differences are small, although r^{-6}_{av} tends to be less than $\langle r^{-6}\rangle$.[21] For $H^{\beta 1}$-$H^{\gamma 1}$ in Met-105, the difference in $\langle r^{-6}\rangle$ and r^{-6}_{av} is 30%. Decreases in the average distances due to motional averaging (i.e., $\langle r^{-6}\rangle > r^{-6}_{av}$) tend to offset the effect of the angular averaging. This is demonstrated in Table II by comparing S^2 with $S^2\langle r^{-6}\rangle / r_{-6av}$. This is not always the case, however; for $H^{\beta 2}$-$H^{\gamma 1}$ of Met-105, a decrease in $\langle r^{-6}\rangle$ when compared with r^{-6}_{av} contributes to a substantial decrease in the cross-relaxation rate.

Interresidue Interactions. The distances to protons on other residues often are comparable to the intraresidue interproton distances. For example, the distance between Trp-108 $H^{\zeta 3}$ and Met-105 $H^{\gamma 2}$ found in the dynamics-average coordinates set is 2.1 Å while the nearest-neighbor ring protons in tryptophan are separated by 2.47 Å. Several interresidue interactions are listed in Table III. The average distances for all of these are less than 3.0 Å. For all of the cases the initial decay of the internal motion correlation function was rapid; the plateau values were generally reached in less than 8 ps. For both the order parameters S^2 and the distance parameter $\langle r^{-6}\rangle$, given in Table III, the motional effects are generally larger than those found within a residue. This is because the interresidue interactions reflect the dynamics of both residues. This can be seen clearly in the coupling between Trp-108 $H^{\zeta 3}$ and the $H^{\gamma 2}$ proton on Met-105. The decrease in the value of $S^2\langle r^{-6}\rangle / r^{-6}_{av}$ observed for this interaction relative to the intraresidue S^2 values for Trp-108 is due largely to the greater mobility of the Met-105 residue. This demonstrates that the relaxation rates coupling protons on relatively immobile residues (e.g., Trp-108) to protons on relatively mobile residues (e.g., Met-105) can be strongly affected by the motions of the mobile residue.

Table IV. Product Approximation for Intraresidue Interactions

^{1}H-^{1}H vector	S^2 product approx (eq 19)	S^2 full dynamics (eq 9)
Trp-28		
$H^{\epsilon 3}$-$H^{\zeta 3}$	0.65	0.86
$H^{\zeta 3}$-$H^{\eta 3}$	0.79	0.83
$H^{\eta 3}$-$H^{\zeta 2}$	0.58	0.79
$H^{\zeta 2}$-$H^{\epsilon 1}$	0.59	0.80
$H^{\epsilon 1}$-$H^{\delta 1}$	0.79	0.88
Trp-108		
$H^{\epsilon 3}$-$H^{\zeta 3}$	0.76	0.92
$H^{\zeta 3}$-$H^{\eta 3}$	0.79	0.91
$H^{\eta 3}$-$H^{\zeta 2}$	0.64	0.90
$H^{\zeta 2}$-$H^{\epsilon 1}$	0.69	0.93
$H^{\epsilon 1}$-$H^{\delta 1}$	0.80	0.91
Ile-98		
$H^{\gamma 11}$-$H^{\gamma 12}$	0.74	0.82
Met-105		
$H^{\gamma 1}$-$H^{\gamma 2}$	0.25	0.35

In some cases interresidue interactions for different pairs of protons on the same two residues can behave differently. This can be seen in the two Trp-108–Met-105 interactions given in Table III, where the difference in $S^2\langle r^{-6}\rangle / r^{-6}_{av}$ is greater than 5%. Deviations of $S^2\langle r^{-6}\rangle / r^{-6}_{av}$ from the value of unity obtained from a static structure range from less than 20% to a 33% decrease. The decrease in $S^2\langle r^{-6}\rangle / r^{-6}_{av}$ for interresidue interactions is on the average larger than that found in either the fixed or variable-distance interactions reported in Tables I and II.

Correlated Motions. The degree of motional averaging predicted from the full dynamics simulation is compared in Table IV with that predicted from averaging separately about the side-chain torsional angles; the latter corresponds to the product approximation (eq 15).[8] For simplicity, cases where the interproton distance is fixed are examined so that only S^2 has to be considered. This comparison shows that the full dynamics simulation predicts considerably less averaging than the product approximation and implies that the motions about side-chain bonds are highly correlated. For Trp-108, for example, only a small degree of motional averaging is found in the full simulation ($S^2 \approx 0.9$ for all proton pairs), but significant averaging occurs in the product approximation ($S^2 \approx 0.64$–0.80). Further, in the full simulation the Trp-108 proton interactions are averaged very differently from comparable interactions on Trp-28. $H^{\zeta 2}$-$H^{\epsilon 1}$ in the full simulation is one of the least motionally averaged interactions on Trp-108, while it is one of the most motionally averaged in Trp-28. By contrast, in the product approximation, $H^{\zeta 2}$-$H^{\epsilon 1}$ is averaged extensively for both residues. The difference between the averaging in the full simulation and the product approximation is a consequence of the degree of correlation of the C^{α}-C^{β}(χ_1) and C^{β}-C^{γ}(χ_2) dihedral angle fluctuations in Trp-108 observed in the simulation. The cross-correlation coefficient for the fluctuations about these two bonds is −0.80 in Trp-108, while the cross-correlation coefficient for Trp-28 is only −0.21.[34]

The difference in the cross-correlation of the torsion angle fluctuations affects the degree of motional averaging and the way specific relaxation rates are averaged for the residues. Even for Trp-28, where the side-chain bond fluctuations are only weakly correlated, the product approximation predicts a decrease in S^2 that is on the average 20% larger than that predicted from the full simulation. This makes clear that for residues in the protein interior the product approximation is likely to be invalid, in contrast to what has been found in model calculations for exterior side chains.[8] This is in accord with a recent molecular dynamics analysis of fluorescence depolarization in the tryptophans of lysozyme.[34]

(34) T. Ichiye and M. Karplus, *Biochemistry*, **22**, 2884 (1983).

Table V

^{1}H-^{1}H vector	S^2 exptl[a,b]	S^2 dynamics
Trp-28 $H^{\epsilon 3}$-$H^{\zeta 3}$	$(0.91 \pm 0.10)_{2.47}$	0.86
$H^{\zeta 3}$-$H^{\eta 3}$	$(0.93 \pm 0.07)_{2.58}$	0.83
Ile-98 $H^{\gamma 11}$-$H^{\gamma 12}$	$(0.46 \pm 0.05)_{1.76}$ $(0.63 \pm 0.08)_{1.85}$	0.82
Met-105 $H^{\beta 1}$-$H^{\beta 2}$	$(0.36 \pm 0.05)_{1.76}$ $(0.49 \pm 0.05)_{1.85}$	0.69

[a] $S^2 = \sigma_{ij}(\text{exptl})/\sigma_{ij}(\text{pred for a rigid molecule with isotropic tumbling; } \tau_0 = 10 \text{ ns})$. [b] The interproton distance used is given as a subscript. For Ile-98 and Met-105 two interproton distances were used; the first (1.76 Å) is obtained from a C-H bond length of 1.08 Å, while 1.85 Å is obtained from a C-H bond distance of 1.12 Å[27] and tetrahedral geometry.

(b) NOE Measurements and Their Interpretation. Dynamical Studies. NOE measurements can be used to obtain motional information for proteins by measuring the rates of direct cross-relaxation (σ_{ij}; see eq 3). This can be achieved by determining the initial rates of the time developments of NOEs.[10] The ratio of the experimental value of σ_{ij} to that estimated for a rigid, isotropically tumbling protein reflects the degree of motional averaging that occurs. For intraresidue protons where the internuclear separation is fixed, the resulting ratio is equal to the order parameter S^2 provided that the internal motions are very fast in comparison to the tumbling time.[10,23] Recently, experimental values of cross-relaxation rates for pairs of protons on three of the four residues considered in this paper have been reported.[10] To estimate S^2 from the experimental cross-relaxation rates it is assumed here that only very fast internal motions are present. Using a value of $\tau_0 = 10 \pm 2$ ns obtained from other experimental data[26,27] and the reported interproton distances,[28,35-39] one obtains the estimates of S^2 reported in Table V.

Despite the uncertainty in S^2 arising from uncertainties in distances and the value of τ_0, a comparison with the predictions from the simulation allows certain conclusions to be drawn. First, the rigidity of the tryptophan rings observed in the simulations ($S^2 \approx 0.9$) agrees with the experimental results for the two pairs of protons studied on Trp-28. Second, the significant degree of motional averaging predicted for proton pairs of Met-105 is observed experimentally. Third, the experimental values of S^2 for Ile-98 and Met-105 are smaller than the values of S^2 predicted by the simulation. This suggests that motions on a time scale long compared with those of the simulation are present and have nonnegligible effects on the cross-relaxation rates. The slower motions are likely to be dihedral angle fluctuations involving transitions between different minima. Since the barriers for such transitions are generally on the order of several kilocalories, their time scale is expected to be in the nanosecond range. For some groups, however, such averaging has been observed in this picosecond simulation. One such case involves χ_2 of Met-105; the dramatic effects of this type of motion on S^2 were seen in Table I.

Structural Studies. The experimental studies of internal motions discussed above made use of fixed-distance interactions to simplify the analysis. If cross-relaxation rates are measured between protons whose distances are not fixed, then one can use the strong distance dependence of σ_{ij} to obtain estimates of the interproton distances.[13,40] This approach has assumed that proteins are rigid and diffuse isotropically so that the NOE-measured distance can be calibrated by using a fixed-distance effect as a standard. It is clearly important to determine whether the picosecond motions are likely to significantly perturb such a correlation. The data from Tables I and II suggest that the effects of the picosecond dynamical processes on the measured distances are small. The angular and radial averaging will change the r^{-6} dependence to a $S^2\langle r^{-6}\rangle$ dependence. The largest change predicted by the ratio of $S^2\langle r^{-6}\rangle/\langle r^{-6}\rangle_{av}$ is 1.0/0.41; this would affect the relative distances by only 20%. In most cases the effects will be less than 20% for measurements up to 5 Å.

Table VI. Simulated Nuclear Overhauser Effects[a]

obsd ^{1}H	r,[b] Å static	−% NOE rigid	−% NOE dynamics
A. Irradiation of Trp-28 $H^{\zeta 3}$ after 100 ms			
Ala-95 $H^{\beta 1-3}$	2.02	45.5	28.5
Trp-28 $H^{\eta 3}$	2.47	11.4	11.0
Trp-28 $H^{\epsilon 3}$	2.53	8.0	8.4
Val-92 H^{α}	2.88	9.3	6.1
Leu-17 $H^{\delta 11-13}$	3.27	4.4	6.0
B. Irradiation of Trp-108 $H^{\zeta 3}$ after 100 ms			
Met-105 $H^{\gamma 2}$	2.08	35.7	25.8
Trp-108 $H^{\eta 3}$	2.47	17.8	14.6
Trp-108 $H^{\epsilon 3}$	2.53	15.7	14.0
Met-105 H^{α}	2.61	19.2	18.9
Leu-56 $H^{\beta 2}$	3.27	5.2	4.1
C. Irradiation of Ile-98 $H^{\gamma 12}$ after 100 ms			
Ile-98 $H^{\gamma 11}$	1.76	53.7	51.0
Ile-98 H^{α}	2.55	11.3	11.4
Ile-98 H^{β}	2.73	7.9	7.6
Ile-98 $H^{\delta 11-13}$	2.35	23.3	21.9
Ile-98 $H^{\gamma 21-23}$	3.15	19.4	17.2
D. Irradiation of Met-105 $H^{\beta 1}$ after 100 ms			
Met-105 $H^{\beta 2}$	1.76	56.8	52.8
Met-105 $H^{\gamma 1}$	2.70	16.2	11.3
Tyr-23 $H^{\epsilon 1}$	2.70	13.4	11.5
Met-105 $H^{\gamma 2}$	2.95	10.7	7.6
Met-105 H^{α}	2.95	9.8	8.4

[a] An irradiation time of 100 ms was used in the simulation; for details of the method see text. [b] Distances from the static dynamics average structure. For methyl groups $r = [\sum_{i=1}^{3} 1/r_i^6]^{-1/6}$, where r_i is the distance between the proton of interest and proton i of the methyl group.

Cross-relaxation rates relevant for longer distance interactions are not directly accessible experimentally in many cases. This is because at short times, when the NOE is proportional to the cross-relaxation rate, the observed NOE for these longer distance interactions are too small to measure accurately. At longer times the NOEs may be observable. However, to analyze such NOEs it is necessary to do a multispin analysis that takes into account secondary NOEs resulting from saturation transfer from protons other than the irradiated proton.[24,25] This approach models all of the relaxation processes that couple the protons with significant NOEs and involves the direct-relaxation rates ρ_i as well as the cross-relaxation rates σ_{ij}.

As described in the methods section, NOEs were calculated by using a multispin approach for the selective irradiation of one proton from each of the four residues considered in this paper. Table VI lists results of these calculations for a rigid model of the protein (with methyl rotation, eq 16) and for a model that includes internal motional averaging calculated from the dynamics simulation. Methyl group rotation was included according to eq 17, and values of σ_{ij} and ρ_i were calculated with eq 12. The data given here are for an irradiation time of 100 ms and include NOEs of the five protons or methyl groups closest to the irradiated proton.

The motional averaging modeled by the dynamics simulation does cause changes in the magnitude of many of the NOEs. For specific cases quite large differences between the models can be

(35) Differences between distances measured from diffraction studies which measure $\langle r\rangle$, and NMR, which depends on $\langle r^{-3}\rangle$, are expected. However, these differences are larger for light atoms bound to heavy atoms, for example, C-H, than for nonbonded proton pairs.[36,37]

(36) L. C. Snyder and S. Meiboom, *J. Chem. Phys.*, **47**, 1480 (1967).

(37) S. Sykora, J. Vogt, H. Bosiger, and P. Diehl, *J. Magn. Reson.*, **36**, 53 (1979).

(38) T. Takigawa, T. Ashida, Y. Sasada, and M. Kukudo, *Bull. Chem. Soc. Jpn.*, **39**, 2369 (1966).

(39) J. C. Speakman, *Mol. Struct. Diffr. Methods*, **2**, 45 (1974), and references therein.

(40) G. Wagner, A. Kumar, and K. Wuthrich, *Eur. J. Biochem.*, **114**, 375 (1981).

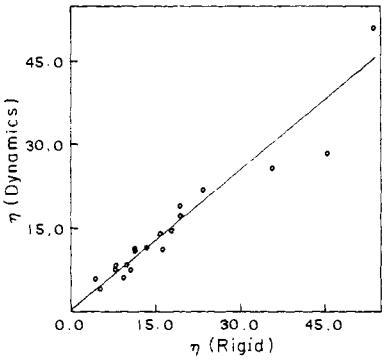

Figure 6. Comparison of NOEs calculated from the dynamics simulation with those calculated from the rigid model (see text). The line is a least-squares fit with a slope of 0.84 and intercept of 0.24.

found. For example, the NOE predicted for $H^{\delta 1}$ of Leu-17 following irradiation of Trp-28 $H^{\beta 3}$ is 50% smaller for the rigid model than the dynamical model. By contrast, the NOE predicted for H^{β} of Ala-95 from the same irradiation is nearly 50% greater for the rigid model than the dynamical model. For intraresidue NOEs the average change is a 10% decrease in magnitude; interresidue NOEs were decreased in magnitude on the average by about 20%. These trends can be seen by plotting the NOEs from the rigid model against those for the dynamical model (Figure 6).

The results from these simulations suggest that the presence of picosecond motions will cause a decrease in the magnitude of most NOEs observed in a protein. However, the decrease is too small to produce a significant change in the distance dependence of most of the NOEs. This is consistent with the strong correlations found between experimental NOE values and distances computed from the crystal structure.[13] However, specific NOEs may be altered by the picosecond motions to such a degree that the effective distances obtained would be considerably different (usually larger) from those predicted for a static structure.

Conclusions

A molecular dynamics simulation of lysozyme has been used to demonstrate that picosecond fluctuations can cause significant changes in the proton relaxation behavior of proteins. Both distance fluctuations and reorientation of the interproton vector play a role in the motional averaging. Changes in the relaxation rates due to internal motions are most readily observable in cases where the cross-relaxation rate between protons separated by a fixed distance can be measured.[10] The reductions in the cross-relaxation rate predicted from the simulations are qualitatively similar to those observed experimentally for the residues examined. However, the consequences of such motional averaging for distance measurements using NOEs are unlikely to be important in most cases; changes of a factor of 2 in the NOE will result in a factor of only 1.2 in distance due to the inverse sixth root dependence of the cross-relaxation rate on the interproton distance.

The present study indicates that care must be taken in the interpretation of the cross-relaxation rates by simple motional models because of the possible effects that correlated motions can have on the averaging of the interaction. The two types of effects that can occur are correlation of dihedral angle fluctuations within a side chain and correlation between the motions of two residues. The importance of correlation effects found here for interior residues is in accord with earlier molecular dynamics analysis of the bovine pancreatic trypsin inhibitor[11,12] and of lysozyme.[34] Corresponding effects have been noted in studies of ring-current contributions to chemical shifts[33] and the depolarization of tryptophan fluorescence.[34]

Acknowledgment. We thank J. C. Hoch and F. M. Poulsen for helpful discussions.

Appendix A

If the limits of integration in eq 11 are extended to infinity, one obtains

$$\int_0^{\infty} [\langle A(t)A(0)\rangle - S^2\langle r_{ij}^{-6}\rangle]\, dt \qquad (A1)$$

(Since $\langle A(t)A(0)\rangle = S^2\langle r_{ij}^{-6}\rangle$ for $t > t_p$, this integral is equal to the integral in eq 11.) An integral of this general form has been used to define an effective correlation time in a recently proposed model-free interpretation of the effect of motions on NMR relaxation data in the extreme narrowing limit.[22,23] Here, for a fixed internuclear distance an effective correlation time, τ_e, is defined by an integral of the form

$$\tau_e(1 - S^2) = \int_0^{\infty} [\langle A(t)A(0)\rangle - S^2]\, dt \qquad (A2)$$

where τ_e is used in the expression for an approximate correlation function (C^A);

$$C^A(t) = [S^2 + (1 - S^2)\exp(-t/\tau_e)]\exp(-t/\tau_0) \qquad (A3)$$

Using this approach, one obtains the resulting spectral density function as[23]

$$J(\omega) = \frac{S^2 r_{ij}^{-6}}{4\pi}\left[\frac{\tau_0}{1 + (\omega\tau_0)^2}\right] + (1 - S^2)r_{ij}^{-6}\left[\frac{\tau_m}{1 + (\omega\tau_m)^2}\right] \qquad (A4)$$

where $\tau_m^{-1} = \tau_0^{-1} + \tau_e^{-1}$. For $\tau_m\omega \ll 1$ and $S^2\tau_m \ll \tau_0$, eq A4 reduces to the result given by eq 12 for fixed-distance interactions.

Registry No. Lysozyme, 9001-63-2.